Effect of Variation of Degree of Saturation with depth on Soil–Concrete Pile Interface in Clayey Soil

Zainal, Abdul Kareem Esmat
Assistant Professor
College of Engineering-University of Baghdad
Email: kareem_esmat@yahoo.com

Abbas, Mohammed Fadhil
Department of Civil Engineering
College of Engineering-University of Baghdad
Email:mhfa1984@yahoo.com

ABSTRACT

Bearing capacity of a concrete pile in fine grained cohesive soils is affected by the degree of saturation of the surrounding soil through the contribution of the matric suction. In addition, the embedded depth and the roughness of the concrete pile surface (expressed as **B**ritish **P**endulum **N**umber **BPN**) also have their contribution to the shear strength of the concrete pile, consequently its bearing capacity. Herein, relationships among degree of saturation, pile depth, and surface roughness, were proposed as a mathematical model expressed as an equation where the shear strength of a pile can be predicted in terms of degree of saturation, depth, and BPN. Relationship among undrained shear strength of the soil, depth and degree of saturation also found and expressed as mathematical equation that represents a 3D- surface; where the value of c_u can be predicted by knowing the other aforementioned factors. Relationship between shear strength and the concrete surface roughness was also shown reflecting that the shear strength increases with the increase of surface roughness.

Keywords: unsaturated soil, shear strength, concrete piles, deep foundation.

تأثير تغير درجة التشبع مع العمق على التماسك بين التربة والركيزة الكونكريتية في التربة الطينية

م.م. محمد فاضل عباس
قسم الهندسة المدنية
كلية الهندسة / جامعة بغداد

ا. م. د. عبد الكريم عصمت زينل
قسم الهندسة المدنية
كلية الهندسة / جامعة بغداد

الخلاصة

سعة التحمل للركائز الخرسانية المستخدمة في الترب ذات الحبيبات الناعمة والتي لها خاصية التماسك تتأثر بشكل كبير بدرجة التشبع لتلك التربة من خلال مساهمة قوى المص الجزيئي. إضافة إلى تأثير كل من عمق الركيزة، ودرجة خشونة سطح الكونكريت معبَّراً عنه بالرقم البندول البريطاني BPN ، من خلال التأثير على قوى تحمل القص. في هذا البحث، تم إيجاد علاقات تجمع بين العوامل المؤثرة وهي درجة التشبع، العمق، والرقم البندول البريطاني من خلال نموذج رياضي على شكل معادلة يمكن من خلالها التنبؤ بإجهاد تحمل القص للركيزة من خلال معرفة العوامل أعلاه.

و تم إيجاد علاقة بين إجهاد التماسك غير المبزول ودرجة التشبع والعمق على شكل معادلة رياضية تمثل سطح ثلاثي الإبعاد يمكن من خلالها التنبؤ بإجهاد التماسك من خلال معرفة باقي العوامل المذكورة. كما تم إيجاد علاقة تربط بين خشونة سطح الكونكريت المستخدم في الركيزة وتحمل إجهاد القص يبين زيادة اجهاد التحمل مع زيادة خشونة سطح الكرنكريت.

كلمات مفتاح: تربة غير مشبعة, مقاومة القص ,الركائز الكونكريتية , الأسس العميقة

1. INTRODUCTION

In geotechnical engineering, classical soil mechanics design are used for the precast concrete pile foundations assuming that the soil is in saturated state. However, in several situations, the soils in natural state are found in an unsaturated state as the water under earth's surface is at a low depth level. This is especially true for soils in barren and semi–barren zones. Almost 40 percent of the natural soils on the earth's surface are in a partially saturated state **Kholghifard, et al., 2012**. Most of the structures and building foundations including piles are constructed in this zone or a mixed zone of saturated / unsaturated conditions, where the shear strength of the unsaturated soil vary significantly and is important to be known.

Shear strength in unsaturated soils based on the suction pressure that varies with the degree of saturation for soil; consequently, that makes the shear strength of the soil varies with degree of saturation. **Fredlund, et al., 1978**.

Interfaces between soil and structure could experience relative motions under static and dynamic loadings. These relative motions include translational, rotational, and rocking motions. The ultimate shaft resistance of pile in unsaturated soil (coarse and fine-grained soils) can be estimated by the modified α and λ methods **Vanapalli,** and **Mohammed, 2007**. The methods listed can be used for determining the change of the friction capacity of the precast concrete pile with respect to suction using the properties of soil in saturated state and Soil Water Characteristic Curve (SWCC).

Vanapalli, and **Taylan, 2012** studied the contribution of matric suction effect on the shaft capacity of single piles. Based on the experimental results, the traditional (λ, α, and β) methods were modified to determine the total shaft resistance of piles in unsaturated soils by including the effect of suction.

Uchaipichat, 2012 showed simulations performed on a pile with diameter of 0.40 m and it length ranges from 5 to 20 m. installed in clay layer (unsaturated state) with matric suction that ranges from 10 to 10,000 kPa. The results show a decrease in matric suction with decreasing pile capacity and factor of safety.

The interface shear strength between concrete and soil is an important design parameter for estimating the bearing capacity of concrete pile. General concept for interface between soil and pile was discussed by many investigators; **Taha, 2010** explored the interface characteristics between a marine clay, steel and concrete investigating the effects of several parameters such as interface roughness, degree of saturation, OCR, dry density and clay salt content. The critical controlling parameter of interface strength was found to be the relative steel surface roughness.

These tests described the minimum residual strength acquired in each test and provided a basis for a arbitrage with other published research. It is demonstrated that the residual strength depends mainly on the material and its roughness, soil properties, and the clay fraction.

2. THEORETICAL BACKGROUND

The reliable determination of soil-structure interaction parameters requires cumbersome laboratory or field tests. Alleviating the need of such cumbersome tests; empirical methods are proposed to estimate the skin friction, *fs* based on the conventional shear strength parameters and the information related to the variation of effective stresses along the length of the piles.

$$fs=f(\sigma'_v, \varphi', c_u) \quad (1)$$

where, σ'_v = vertical effective stress, φ'= effective friction angle, and c_u = undrained shear strength. Eq. (1) suggests that the skin friction, *fs* can be analyzed in terms of either total or

effective stress approach considering the loading and drainage conditions (i.e., *TSA* or *ESA*), respectively.
Experimental programs were planned to determine the contribution of matric suction on the shaft resistance and not the end bearing resistance.

The λ-method is an empirical method, based on effective stresses induced in the soil and total soil strength (calculated from undrained shear strength). This method may be used to relate the unit skin friction to the passive earth pressure. The value of λ was empirically-determined by examining the results obtained from various load tests conducted on piles in cohesive soils. Therefore, this method is more accurate, if used for the same soil and pile conditions.

The λ - method combines the total (i.e., undrained) and effective (i.e., drained) stress approaches for determining the shaft capacity of driven piles into cohesive soils **(Vijayvergiya and Focht, 1972)**. This technique is useful in reducing the sensitivity of the shear strength parameters measured using the total stress and effective stress approaches. Eq. (3.10) was used to calculate the skin friction for saturated condition:

$$Q_f = \lambda(\sigma_v' + 2cu)\pi dl \quad (2)$$

λ = frictional capacity coefficient which is a function of entire embedded depth of pile.
Only one method (α-method will be considered in this work to demonstrated the effect of depth of pile and degree of saturation on the soil-concrete pile interface), for other methods refer to Abbas, Mohammed F., 2015).

2.1 The α Method

The α-method is a semi-empirical approach of calculating the pile skin friction, based on the total stresses induced in the soil and calculated using the soil's undrained shear strength (c_u). This method was mainly developed for cohesive soils. It has been used for many years and has proven to provide reasonable design capacities for piles.
This method depends on the alpha factor (α), which is indirectly related to the soil's undrained shear strength (c_u). The factor was back calculated from several pile load tests. The ultimate shaft capacity of a pile, Q_f is dependent on the undrained shear strength, c_u in soil adjacent to the foundation. The unit skin resistance, f_s can be expressed as in Eq. (2) using undrained shear strength, c_u.

$$f_s = \alpha c_u \quad (2)$$

The adhesion factor, α is not constant but decreases with increasing undrained shear strength, c_u of the soil and varies from close to unity for low strength soft clays and reach almost to a value of 0.4 for stiff clays **Tomlinson, 1957** and **Skempton, 1959**. The ultimate shaft capacity, Q_f for cylindrical piles using the α method can be estimated as in Eq. (3).

$$Q_f = f_s \times A_s = \alpha c_u \pi dl \quad (3)$$

where, d = pile diameter, and l = length of pile.
The adhesion factor, α can be computed from API (1984). Eq. (4) can be used for estimating the α value.

$$\alpha = 1.0 \qquad \text{for } cu < 25kPa$$
$$\alpha = 1.0 - 0.5\left(\frac{cu - 25}{50}\right) \qquad \text{for } 25kPa < cu < 75kPa \qquad (4)$$
$$\alpha = 0.5 \qquad \text{for } cu > 75kPa$$

2.2 Modified α Method

Several investigators related the load bearing capacity of a single pile to the undrained shear strength, c_u of the cohesive soils **Tomlinson, 1957, Dennis,** and **Olsen , 1983**. Eq. (5) given by **Oh** and **Vanapalli, 2009** can be used to estimate the variation of undrained shear strength with respect to matric using the *SWCC* and undrained shear strength for saturated condition, $cu_{(sat)}$.

$$c_{u(unsat)} = c_{u(sat)}\left[1 + \frac{(u_a - u_w)}{(P_a/101.3)}\left(s^v\right)\Big/\mu\right] \qquad (5)$$

where, $c_{u(sat)}$ and $c_{u(unsat)}$ = undrained shear strength under saturated and unsaturated conditions, respectively, P_a = atmospheric pressure (i.e. 101.3 kPa), and v and μ are fitting parameters.
The fitting parameter v depends on the soil type (i.e., coarse or fine-grained soils) and is equal to 1 for coarse-grained soils and 2 for fine-grained soils. The fitting parameter μ however is a function of plasticity index, *PI*.

$$\mu = 9 \qquad (8 \le PI(\%) \le 15.5) \qquad (6)$$

$$\mu = 2.1088\, e^{0.0903PI} \qquad (15.5 \le PI(\%) \le 60) \qquad (7)$$

The ultimate shaft capacity of piles in unsaturated soils as given below.

$$Qf_{(unsat)} = \alpha c_{u(sat)}\left[1 + \frac{(u_a - u_w)}{(Pa/101.3)}\left(s^v\right)\Big/\mu\right]\pi dl \qquad (8)$$

The undrained shear strength under saturated condition, $cu_{(sat)}$ and the *SWCC* are required to estimate the variation of ultimate shaft capacity of pile, $Qf_{(unsat)}$ with respect to matric suction.

3. SOIL PROPERTIES

Soil samples were collected from one site within AL–Muthanna governorate from Samawah city region. The physical properties of this soil was studied by conducting series of tests in the laboratory, these tests included: Specific gravity, Grain size distribution, Atterberg limits, Direct shear test, and Interface between clayey soil and concrete pile surface by modified direct shear box test. For each sample, the matric suction was measured using the filter paper technique (Whatman No.42) at different degrees of saturation. Atterberg limits and other soil properties values are summarized in Table (1) and grain size distribution is shown in **Fig.1**.

4. Experimental Program

Soil samples were collected from one site within AL–Samawah city region from depth (3.7 m – 4.5 m). These samples were subjected to testing program that included the following tests:

4.1 Direct Shear Box Test

Direct shear tests were carried out after remolding the samples in accordance with ASTM D3080. Different loading was used to find the shear strength of the sample soil at failure according to the following assumption:

1- A typical pile of 6m depth is assumed for this study.
2- Three places through the pile depth were examined to identify the strength of the soil-pile interface; these places are at the depths of 2m, 4m, and 6m from soil surface.
3- Normal stresses to the pile surface were computed at these three places regarding different unit weight conditions of the soil; low, natural, and high representing low unit weight, normal unit weight (as in situ), and high unit weight, this reflects low, natural and high value. K_o value was computed according to **Das, 2002**, where he suggested that for fine grained, normally consolidated soils, the following Eq.(9) for K_o can be used :

$$K_o = 0.44 + 0.42(PI\%/100) \quad (9)$$

where:
K_o = the coefficient of lateral earth pressure at rest,
PI = plasticity index
PI value for the soil is, PI = 20%
$\therefore K_0 = 0.525$

$$\text{Normal stress for direct shear test} = \gamma \times h \times K_o \quad (10)$$

So each sample was sheared till reaching failure for three normal stresses: 17 kPa, 22 kPa, and 24 kPa for the depth of 2m and 34KPa, 44KPa, 48 kPa for the depth of 4 m and 50.5 kPa, 66KPa, 72.5 kPa for the depth of 6m depth respectively.

4- The undrained shear strength (c_u) of each sample was measured by carrying out direct shear test through remolding the sample at different degrees of saturation (100%, 90%, 80%, 70%, and 60%) (Smaller values of degree of saturation gave insignificant contribution to the results).

4.2Matric Suction of soil by filter paper method

The filter paper method has long been used in soil science and engineering practice and it has recently been accepted as an adaptable test method for soil suction measurements because of its advantages over other suction measurement devices. Basically, the filter paper comes to equilibrium with the soil either through vapor (total suction measurement) or liquid (matric suction measurement) flow. At equilibrium, the suction value of the filter paper and the soil will be equal. After equilibrium is established between the filter paper and the soil, the water content of the filter paper disc is measured. Then, by using filter paper water content versus suction calibration curve, the corresponding suction value is found from the curve. This is the basic approach suggested by ASTM Standard Test Method for Measurement of Soil Potential (Suction) Using Filter Paper (ASTM D 5298), the results are shown in **Fig.2**.

4.3Pile Interfaces

The interface roughness between the soil and pile material plays an important role in determining the frictional strength capacity along the shaft of the concrete pile. In this study, three concrete materials pile interface were taken into consideration with roughness for each one.

The effect of the roughness is studied in order to establish a relationship between the shear strength property for the clayey soil and the concrete pile surface roughness. Micro roughness is relevant at the scale of the particle size of the soil being sheared against the surface.

Surface roughness was measured using **The British Pendulum Number (BPN),** the British pendulum tester is one of the simplest and cheapest instruments used in the measurement of friction characteristics of pavement surfaces. The British Pendulum Number (BPN) values for the three concrete materials are shown in Table 2.

The CBPN65 interface was taken from the precast concrete pile's body by cutter with dimensions (5.8×5.8) cm which placed in lower half of the shear box. The other two concrete samples were prepared by using a pre-mixed cement-fine sand grout with a 1:3 ratio of sand to cement, and 40% water cement ratio by weight. The samples were cast in the lower portion of a shear box device with different face roughness, and allowed to cure for 14 days prior to initial testing. **Fig. 3** and **Fig. 4** show the concrete–soil interface before and after the test respectively.

4.4Experimental Procedure

The interface characterization program was carried out using a direct shear test apparatus (ASTM D3080/D3080M, 2012). The direct shear test apparatus consists of a displacement controlled testing apparatus used to apply a fixed displacement rate to the shear box device through a series of gearing mechanisms. The shear box has inside specimen dimensions of 60×60 mm, outside dimensions of 90×90 mm and a specimen height of 25.4 mm. schematic drawing of the shear box is shown in **Fig. 5** and the device is shown in **Fig. 6**.

The normal pressure is applied by a steel bearing arm using weights to apply vertical stresses to the specimen. The shearing stresses are measured through a digital load cell connected horizontally to the top section of the shear box.

Horizontal and vertical displacements are measured through linear variable differential transducer (LVDT) connected to a digital logging station using Lab View software. The shear box device was slightly modified by replacing the lower half of the standard direct shear box with the interface material for interface tests.

4.5Testing Procedure

Interface testing was carried out in accordance with ASTM D3080/D3080M (2012). The modified shear box device was placed within a metal container which was laid upon a set of linear ball bearings allowing unrestricted horizontal displacements. The normal loading was applied through a steel bearing arm connected to the top section of the shear box.

Three different normal pressures of (17, 22 and 24) kPa for 2m depth, (34, 44, and 48) kPa for the 4m depth, and (50.5, 66, and 72.5) kPa for the 6m depth were applied to simulate typical lateral earth pressures along the pile shaft at a moderate driving depth.

The shearing rates applied were achieved through the use of a precise screw type actuators calibrated to 2.5 mm/min in order to simulate undrained condition.

5. Results of the Experimental Tests

The undrained shear strength (c_u) of soil was measured by carrying out direct shear test through remolding the samples at different degree of saturation (100%, 90%, 80%, 70%, and 60%). The results demonstrate that the undrained shear strength (c_u) increases with the decrease of the degree of saturation (S), while the angle of internal friction (Ø) is found to be very small and had very small effect especially with clayey soils; this was also noticed by **Fredlund and Rahardjo, (1993).** The results of direct shear test (undrained and unconsolidated) are shown in table 3 and graphically in **Fig. 7**.

5.1 Direct Shear Test for (Clay–Concrete) Samples

Direct shear tests were conducted on the three concrete materials. Through these tests, it is required to determine the shear strength of the clay–concrete interface and to determine the location of failure from direct observations.

Split samples are prepared having one half filled with concrete and the other half is filled with soil. The direct shear test results (undrained condition) are shown in **Fig.8 to Fig. 10.**

5.2 Estimation of the Ultimate Shaft Capacity of Concrete Pile in unsaturated Fine soil by α Method.

The modified α method was used to estimate the ultimate shaft capacity of a single pile in unsaturated undrained condition, implementing modified direct shear test for concrete pile's surface, and three different depths. The modified α is proposed in a functional form such that it can be used to predict the variation of shaft capacity of the pile with respect to matric suction under undrained loading conditions.

Similar to the approach used for saturated soils, the ultimate shaft capacity of a pile is related to the undrained shear strength, c_u by introducing a dimensionless parameter which is the adhesion factor, α. In other words, the method is based on the total stress approach based on Eq. (8) for estimate shaft capacity of concrete pile. Results are show in table 4 to table 6 for CBPN49, from table 7 to table 9 for CBPN52, and from table 10 to table 12 for CBPN56 respectively. Graphical representations of these tables are shown in figure 11 to 19 respectively with the tables.

6. DISCUSSION

Regarding the experimental data results obtained from the tests conducted on the samples of soil and soil–concrete combinations that describe the interaction between the soil and the pile surface material it can be noted that:

6.1 Variation of the Undrained Shear Strength with Depth and Degree of Saturation.

From Table (3) and **Fig.7** it can be noted that there is a variation in the undrained shear strength of the soil with depth and the degree of saturation. This relationship can be described as a surface represented in **Fig.20**. This surface may describe the variation of the undrained shear strength of the soil with depth and degree of saturation. The increase of the undrained shear strength with decreasing degree of saturation was noticed by many investigators **Nishimura** and **Vanapalli, 2004, and Fattah, et al., 2012** and is explained due to the contribution of the matric suction to the shear strength. The increase of undrained shear strength with increasing depth may be explained as the contribution of overburden pressure that may increase the effect of adhesion factor due to increasing the confining pressure with depth, hence affecting the angle of friction δ' and increasing the factor tan δ'. However, since the soil used is a cohesive fine grained soil, the contribution of (tan δ') is observed to be very small compared to the contribution of the degree of saturation S. A proposed relationship was found through curve fitting computer programs, as in Eq. (11), with R^2=0.989, and shown in **Fig.21.**

$$c_u = \frac{S - 159.3}{0.002758D^2 - 1.07} - \frac{2850}{S} \quad (11)$$

where S = Degree of Saturation in percent, D = Depth in meters.

6.2 Failure Location

To determine the failure location that may occur under loading, it is necessary to determine the weaker shear stress resistance between the soil itself (c_u) and the adhesive bonds at

the interface between the soil and the concrete. Since these stresses vary with the degree of saturation, the study of these variations are important to determine the failure location (i.e. soil failure or interface failure). Results for three depths of (e.g. CBPN65) are shown in **Tables (13, 14, and 15)** and represented graphically in **Fig.13, 14 and 15**.

It can be observed generally that the value of (c_u) is low at lower degrees of saturation and high at higher degrees of saturation, in opposite to the value of τ where it could be observed to be low at higher degrees of saturation and high at lower degrees of saturation for all of the three depths shown (i.e. 2m, 4m, and 6m). A transient range can be observed between about S=75% to 85% that the lower values between c_u and τ change places.

The failure usually occurs when the weaker value of the shear resistance is reached, and since the weaker value changes with the degree of saturation then it is worth to note that the correct value of the shear resistance should be used during design depending on the degree of saturation. Varying degree of saturation during seasons makes it unavoidable for the designer to establish a relationship between the weaker shear resistance and the degree of saturation for the soil type, and pile surface roughness used for the pile foundation design.

7. Conclusions

Trying to predict relationships among many factors that may affect the carrying capacity of a concrete pile foundation could help in adding a more clear vision of pile use (design or analysis) from economical or strength points of view in unsaturated soils.

Factors like the degree of saturation (S), length of a pile (D), and roughness of the pile surface expressed as **B**ritish **P**endulum **N**umber (BPN) were found to have good contribution in affecting the shear strength of a frictional pile, these contributions were expressed mathematically and many conclusions may be expressed herein.

1. Undrained shear strength of soil related to the depth and degree of saturation was obtained as a surface, and expressed as a mathematical model shown by Eq. (11).
2. Equations describing the shear strength of pile foundations were found to be very helpful in predicting the shear strength for unsaturated soils regarding the contribution of the matric suction. These equations can be used to express the shear strength for cohesive soils that may exhibit adhesive bonds between pile surface and fine grained soils like clayey soils.
3. The concrete of the pile surface gave greater shear strength for the rougher surface (BPN49) and became lesser for the softer surface (BPN65). This observation proves the contribution of the surface roughness to the shear strength of the pile.
4. Failure location (where the failure occurs either in the soil material or in the interface part between the soil and the pile surface) was found to be affected by the degree of saturation. Failure location was noticed to occur in the soil material for the degree of saturation less than about 75% and the failure was noticed to occur at the soil–material interface for the degree of saturation greater than about 85%. Degree of saturation between about 75% – 85% was found to be a transient range where the failure type changes from failure type to another.
5. Since CBPN49 and CBPN52 were molded concrete and CBPN65 was already taken from precast pile, it can be roughly concluded that precast piles are smoother than the cast in place piles. This may increase the contribution of the adhesive bonds (and also frictional part in c–ϕ and ϕ soils) and consequently the shear strength and bearing capacity of the pile.

REFRENCES

- Abbas, Mohammed F., 2015, "Effect of Variation of Degree of Saturation with depth on Soil – Concrete Pile Interface in Clayey soil", Thesis submitted to the college of Engineering / Baghdad University / Civil Engineering Dept.
- API (1984). Recommended Practice for Planning Designing and Construction Fixed Offshore Platforms, 14th Edt. APIRP2A, American Petroleum Institute, Dallas, TX.
- Das, B.M., (2002), *Principles of Geotechnical Engineering*, fifth edition, wadsworth group,pp.340.
- Dennis, N.D.; Olsen, R.E.,(1983), "Axial capacity of steel pipe piles in clay," in Proc. Geotechnical Practice in Offshore Engineering. ASCE, pp. 370-388.
- Fredlund, D.G., Morgenstern, and Wider, R.A.,(1978), *The Shear Strength of Unsaturated Soil*, Canadian Geotechnical Journal,Vol.15,pp.313-321.
- Kholghifard, M. A., Kamarudin A., and Nima, L., 2012, *The Influence of Suction Changes on Collapsibility and Volume Change Behavior of Unsaturated Clay Soil***,** Electronic Journal of Geotechnical Engineering, Vol. 17, pp 2623-2631.
- Oh, W.T.; Vanapalli, S.K.,(2009), "A simple method to estimate the bearing capacity of unsaturated fine-grained soils," in Proc. 62nd Canadian Geotechnical Conf & 10thJoint CGS/IAH-CNC Groundwater Conf., pp. 234-241.
- Skempton, A.W., (1959), "Cast-in-situ bored piles in London clay," Geotechnique, vol. 9, pp. 153-173.
- Taha, A. M.,(2010), *Interface Shear Behaviour of Sensitive Marine Clay - Leda Clay*, M.Sc. Thesis, University of Ottawa, Ottawa, Ontario, Canada.
- Tomlinson, M.J.,(1957), "The adhesion of piles driven in clay soils," in Proc. 4th Int. Conf. on Soil Mech. and Foundation Eng., vol. 2, pp. 66-71.
- Uchaipichat, A. (2012). *Variation of Pile Capacity in Unsaturated Clay Layer with Suction*, Electronic Journal of Geotechnical Engineering,Vol.17,pp.2425-2433.
- Vanapalli, S.K. and Mohamed, F. M. O.,(2007), *Bearing Capacity of Model Footing in Unsaturated Soils,* In Experimental Unsaturated Soil Mechanics, Springer Proceeding in physics, Springer- Verlag Berlin Geidelberg, Vol. 112, pp.483-493.
- Vanapalli, S.K. ,(2009), *Shear strength of unsaturated soils and its applications in geotechnical engineering practice*, Proceedings of the 4th Asia-Pacific Conference on Unsaturated Soils. New Castle, Australia. Nov. 23-25, 2009,pp.579-598.
- Vanapalli S.K. and Taylan Z.N.,(2012), *Design of Single Piles Using the Mechanics of Unsaturated Soils*, Int. J. of GEOMATE, Vol. 2, No. 1 (Sl. No. 3), pp. 197-204.
- Vijayvergiya, V.N.; Focht, J.A.,(1972), "A new way to predict capacity of piles in clay," in Proc. Offshore technology Conf., pp. 865-871.

SYMBOLES

μ= fitting parameter, dimensionless.
A= area , m^2
BNP= british pendulum number, dimensionless.
C_a= adhesion component of cohesion, kPa.
c_u= undrined shear strength ,kN/m^2.
D= depth of pile, m^2
e= void ratio, dimensionless.

Gs= specific gravity, dimensionless.
k_o= the coefficient of lateral earth pressure at rest, dimensionless.
L.L= liquid limit, dimensionless.
P.I= plasticity index, dimensionless.
P.L= plastic limit, dimensionless.
p_a = atmospheric pressure, kPa.
Q_f = carrying load capacity, kPa.
S= degree of saturation, dimensionless.
u_a-u_w =matric suction, kPa .
USCS= unified soil classification system.
v= fitting parameter, dimensionless.
α = adhesion factor, dimensionless.
γ= unit weight, kN/m^3
τ= shear stress ,kN/m^2.
τ_f = shear stress at failure, kPa.
ϕ = internal friction angle ,degree.
δ' = internal friction angle between pile and soil, degree.
h = height, m.
d= pile diameter, m.

Table 1. Properties of used soil.

PROPERTY	***VALUE***
Liquid limit % (L.L)	39
Plastic limit % (P.L.)	19
Plasticity index % (P.I.)	20
Specific gravity(Gs)	2.79
Natural degree of saturation (S%)	100
Clay %	67.5
Void ratio,(e_o)	0.644
Total Unit weight (kN/m^3)	20.93
Natural moisture content %	23.3
Classification according to (USCS)	CL

Table 2. Values of Pile interface British Pendulum Number, average roughness, and name used.

Interface Surface	BPN	**Ra(μm)**	Name Used in This Research
Concrete (1)	49	25	CBPN49
Concrete (2)	52	23.7	CBPN52
Concrete (3)	65	21.2	CBPN65

Table 3 Results of direct shear test on remolded samples at different degrees of saturation.

Depth(m)	**S (%)**	**c_u(kPa)**
2	100%	10.3
	90%	35.24
	80%	45.74
	70%	53.61
	60%	60.42
4	100%	13.11
	90%	39.9
	80%	48.77
	70%	61.17
	60%	66.5
6	100%	15.9
	90%	48.31
	80%	52.57
	70%	70.6
	60%	73.29

Table 4 . Estimated and measured ultimate shaft capacity for CBPN49 surface using the modified α method at depth (2) m.

S	u_a-u_w	$C_{u(sat)/unsat.}$ ***Meas.***	***μ***	***v***	***α***	***Back Cal. α value***	$\tau_{f(us)}$ ***Est.***	$\tau_{f(us)}$ ***Meas.***
%	**kPa**	**kPa**	**----**	**-----**	**-----**		**kPa**	**kPa**
100	0	10.3	13	2	1	1.05	10.3	10.81
90	49.2	35.24	13	2	0.83	0.76	35.28	31.9
80	107.7	45.74	13	2	0.61	0.69	39	45.2
70	221	53.61	13	2	0.5	0.64	48.1	61.9
60	319	60.42	13	2	0.5	0.66	50.64	67.42

Table 5. Estimated and measured ultimate shaft capacity for CBPN49 surface using the modified α method at depth (4) m.

S	u_a-u_w	C_u meas.	μ	ν	α	Back Cal. α value	$\tau_{f(us)}$ Est.	$\tau_{f(us)}$ Meas.
%	kPa	kPa	----	-----	-----		kPa	kPa
100	0	13.11	13	2	1	1.1	13.11	14.5
90	49.2	39.9	13	2	0.71	0.69	38.3	37.1
80	107.7	48.77	13	2	0.5	0.6	41.3	49.8
70	221	61.17	13	2	0.5	0.605	61.16	73.9
60	319	66.5	13	2	0.5	0.61	64.4	78.38

Table 6. Estimated and measured ultimate shaft capacity for CBPN49 surface using the modified α method at depth (6) m.

S	u_a-u_w	C_u meas.	μ	ν	α	Back Cal. α value	$\tau_{f(us)}$ Est.	$\tau_{f(us)}$ Meas.
%	kPa	kPa	----	-----	-----		kPa	kPa
100	0	15.9	13	2	1	0.92	15.9	17.3
90	49.2	48.31	13	2	0.6	0.66	39.4	42.8
80	107.7	52.57	13	2	0.5	0.55	50.1	55.22
70	221	70.6	13	2	0.5	0.54	74.17	81.19
60	319	73.29	13	2	0.5	0.548	78.18	85.79

Table 7. Comparison between the measured and estimated ultimate shaft capacities for CBPN52 surface using the modified α method at depth 2 m.

S	u_a-u_w	$C_{u(sat)/unsat.}$ Meas.	μ	ν	α	*Back Cal. α Value*	$\tau_{f(us)}$ Est.	$\tau_{f(us)}$ Meas.
%	kPa	kPa	----	-----	-----		kPa	kPa
100	0	10.3	13	2	1	0.98	10.3	10.1
90	49.2	35.24	13	2	0.83	0.73	35.28	30.71
80	107.7	45.74	13	2	0.61	0.65	39	42.63
70	221	53.61	13	2	0.5	0.62	48.1	60.28
60	319	60.42	13	2	0.5	0.63	50.64	63.91

Table 8. Comparison between the measured and estimated ultimate shaft capacities for CBPN52 surface using the modified α method at depth (4)m.

S	u_a-u_w	C_u meas.	μ	ν	α	*Back Cal. α Value*	$\tau_{f(us)}$ Est.	$\tau_{f(us)}$ Meas.
%	kPa	kPa	----	-----	-----		kPa	kPa
100	0	13.11	13	2	1	1.06	13.11	14.01
90	49.2	39.9	13	2	0.71	0.69	38.3	36.7
80	107.7	48.77	13	2	0.5	0.55	41.3	46.22
70	221	61.17	13	2	0.5	0.56	61.16	69.09
60	319	66.5	13	2	0.5	0.55	64.4	71.94

Table 9. Comparison between the measured and estimated ultimate shaft capacities for CBPN52 surface using the modified α method at depth (6) m.

S	u_a-u_w	C_u meas.	μ	ν	α	*Back Cal. α Value*	$\tau_{f(us)}$ Est.	$\tau_{f(us)}$ Meas.
%	kPa	kPa	----	-----	-----		kPa	kPa
100	0	15.9	13	2	1	1.03	15.9	16.46
90	49.2	48.31	13	2	0.6	0.62	39.4	40.1
80	107.7	52.57	13	2	0.5	0.48	50.1	47.9
70	221	70.6	13	2	0.5	0.5	74.17	75.13
60	319	73.29	13	2	0.5	0.52	78.18	82.39

Table 10. Comparison between the measured and estimated ultimate shaft capacities for CBPN56surface using the modified α method at depth 2 m.

S	u_a-u_w	$c_{u(sat)}/_{unsat}$ meas.	μ	ν	α	*Back Cal. α Value*	$\tau_{f(us)}$ Est.	$\tau_{f(us)}$ Meas.
%	kPa	kPa	----	-----	-----		kPa	kPa
100	0	10.3	13	2	1	0.96	10.3	9.98
90	49.2	35.24	13	2	0.83	0.72	35.28	30.1
80	107.7	45.74	13	2	0.61	0.87	39	40.86
70	221	53.61	13	2	0.5	0.6	48.1	58.33
60	319	60.42	13	2	0.5	0.62	50.64	63.29

Table 11. Comparison between the measured and estimated ultimate shaft capacities for CBPN56 surface using the modified α method at depth (4) m.

S	u_a-u_w	C_u meas.	μ	ν	α	*Back Cal. α Value*	$\tau_{f(us)}$ Est.	$\tau_{f(us)}$ Meas.
%	kPa	kPa	----	-----	-----		kPa	kPa
100	0	13.11	13	2	1	0.97	13.11	12.74
90	49.2	39.9	13	2	0.71	0.67	38.3	36.16
80	107.7	48.77	13	2	0.5	0.54	41.3	44.97
70	221	61.17	13	2	0.5	0.55	61.16	67.32
60	319	66.5	13	2	0.5	0.549	64.4	70.78

Table 12. Comparison between the measured and estimated ultimate shaft capacities for CBPN56 surface using the modified α method at depth (6)m.

S	u_a-u_w	c_u meas.	μ	ν	α	*Back Cal. α Value*	*f(us)* Est.	*f(us)* Meas.
%	kPa	kPa	----	-----	-----		kPa	kPa
100	0	15.9	13	2	1	0.88	15.9	14.11
90	49.2	48.31	13	2	0.6	0.58	39.4	37.96
80	107.7	52.57	13	2	0.5	0.57	50.1	57.26
70	221	70.6	13	2	0.5	0.504	74.17	74.77
60	319	73.29	13	2	0.5	0.507	78.18	79.34

Table 13.Comparison between values (c_u and measured τ) at 2 m depth CBPN65.

Depth m	**S**	**$c_{u(sat)}/_{unsat.}$ Meas.**	**$\tau_{f(us)}$ Meas.**
	%	kPa	kPa
2	100	10.3	9.98
	90	35.24	30.1
	80	45.74	40.86
	70	53.61	58.33
	60	60.42	63.29

Table 14.Comparison between values (c_u and measured τ) at 4 m depth CBPN65.

Depth m	S	c_u meas.	$\tau_{f(us)}$ Meas.
	%	kPa	kPa
4	100	13.11	12.74
	90	39.9	36.16
	80	48.77	44.97
	70	61.17	67.32
	60	66.5	70.78

Table 15.Comparison between values (c_u and measured τ) at 6 m depth CBPN65.

Depth m	**S**	**c_u meas.**	**$\tau_{f(us)}$ Meas.**
	%	kPa	kPa
6	100	15.9	14.11
	90	48.31	37.96
	80	52.57	57.26
	70	70.6	74.77
	60	73.29	79.34

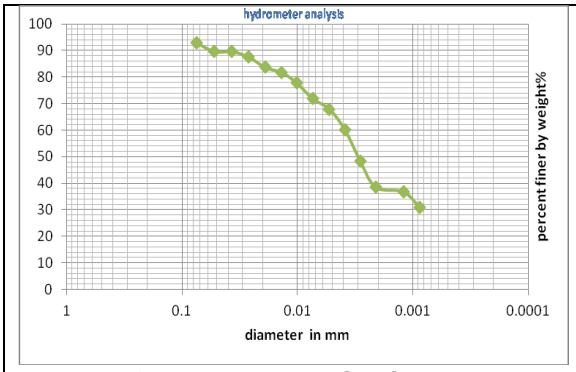

Figure 1. Grian size distribution**.**

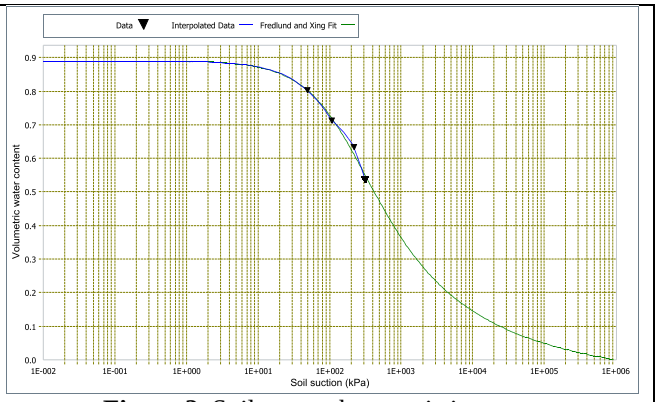

Figure 2. Soil water characteristic curve.

Figure 3. Concrete Interface surface

Figure 4. Concrete–Soil Interface after Failure

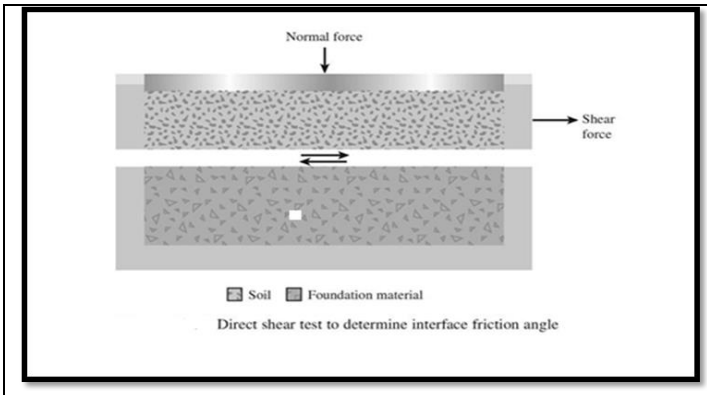

Figure 5. Modified shear box schematic

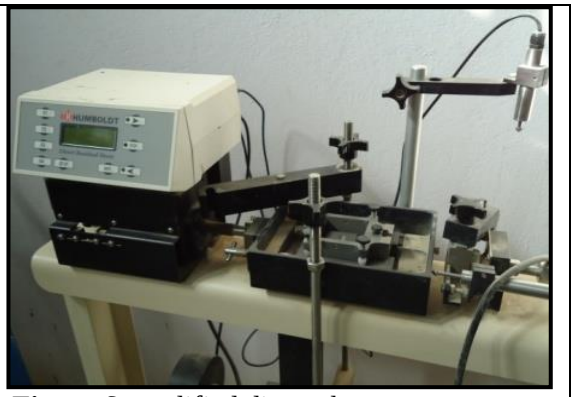

Figure 6. modified direct shear test apparatus

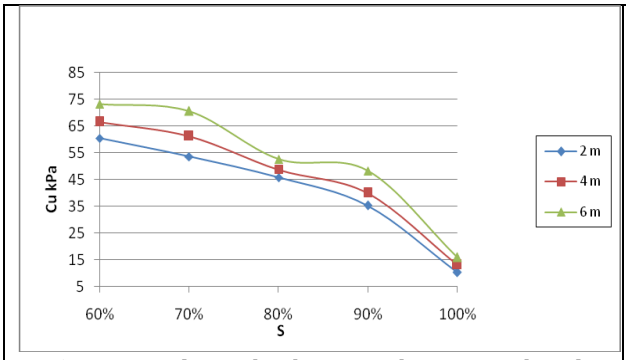

Figure 7. Relationship between shear strength and degree of saturation with different depths.

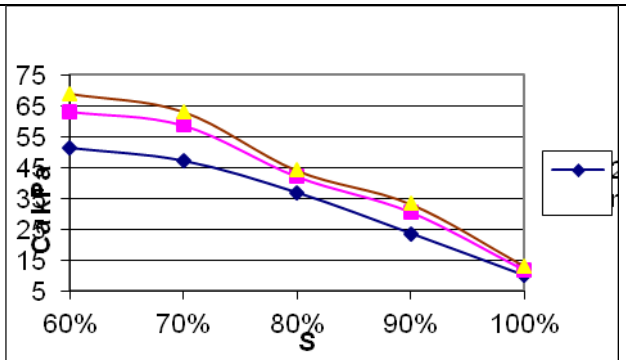

Figure 8. Relationship between adhesion and degree of saturation at different depths for CBPN49 surface.

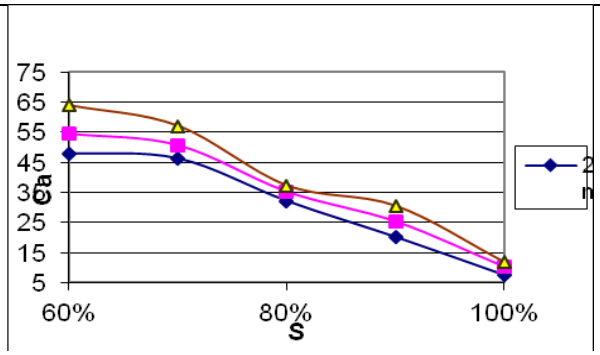

Figure 9. Relationship between adhesion and degree of saturation at different depths for CBPN52surface.

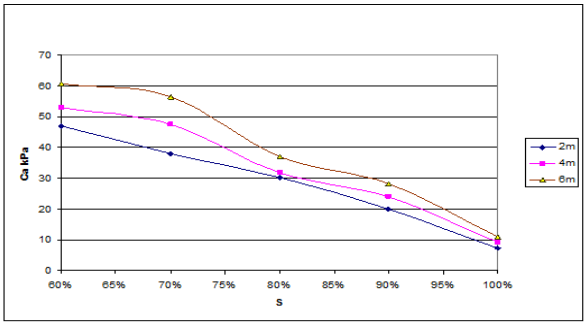

Figure 10. Relationship between adhesion and degree of saturation at different depths for CBPN56surface.

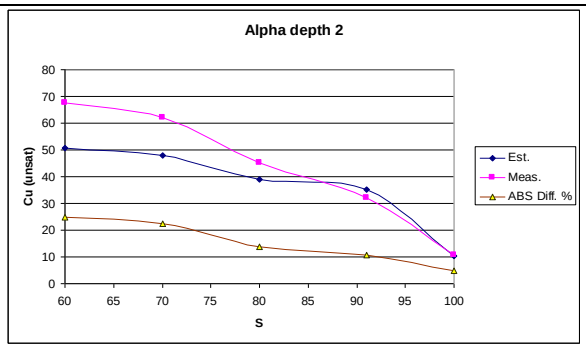

Figure11. Relationship between shear stress(Est. and Meas.) and degree of saturation for CBPN49by using the modified α method with depth (2)m.

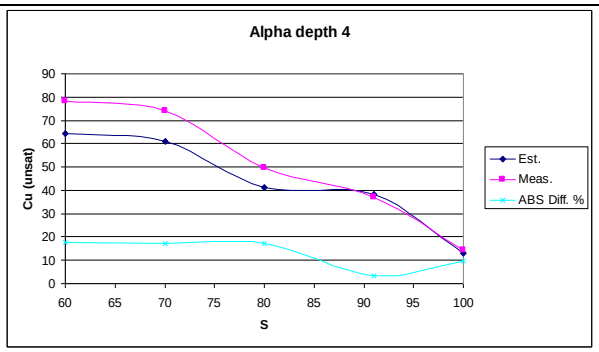

Figure12. Relationship between shear stress(Est. and Meas.) and degree of saturation for CBPN49by using the modified α method with depth (4)m.

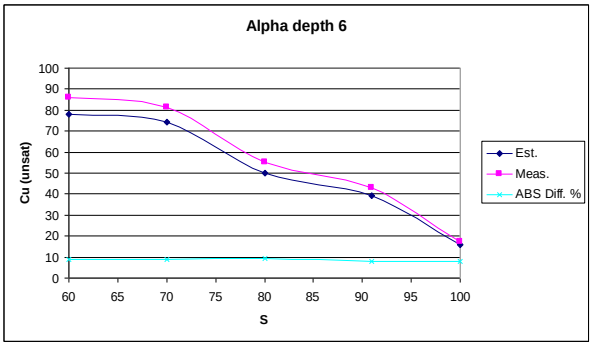

Figure 13. Relationship between shear stress(Est. and Meas.) and degree of saturation for CBPN49by using the modified α method with depth (6)m.

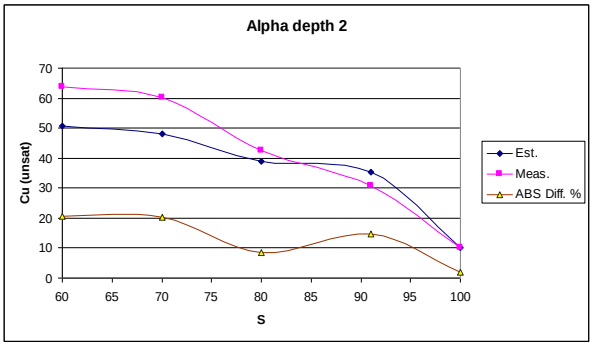

Figure 14. Relationship between shear stress (Est. and Meas.) and degree of saturation for CBPN52 surface

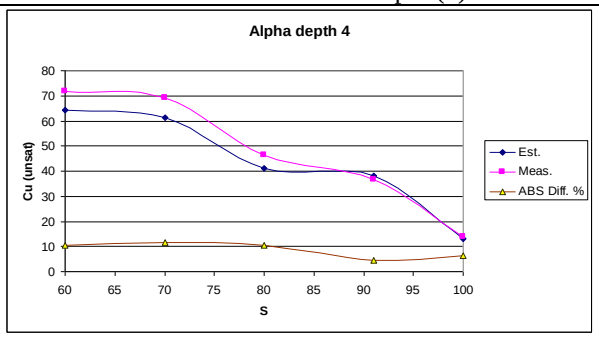

Figure 15.Relationship between shear stress (Est. and Meas.) and degree of saturation for CBPN52 surface

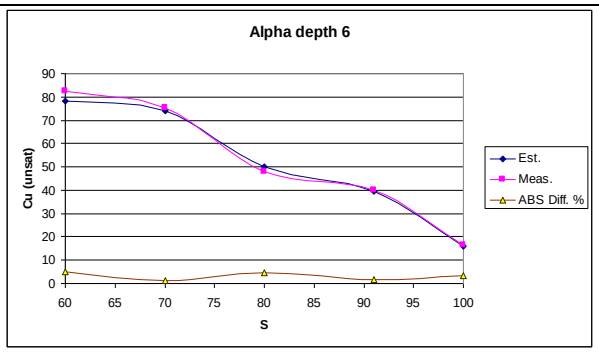

Figure16. Relationship between shear stress (Est. and Meas.) and degree of saturation for CBPN52 surface

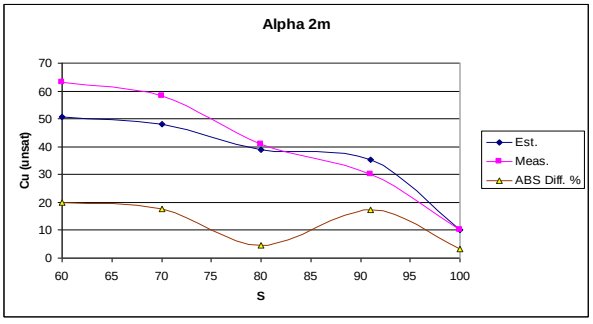

Figure 17. Comparison between estimated and measured shear stress values with different degree of saturation by α method at 2 m depth CBPN56.

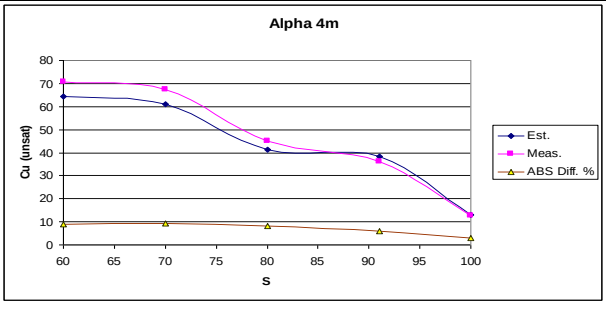

Figure 18. Comparison between estimated and measured shear stress values with different degree of saturation by α method at 4 m depth CBPN56.

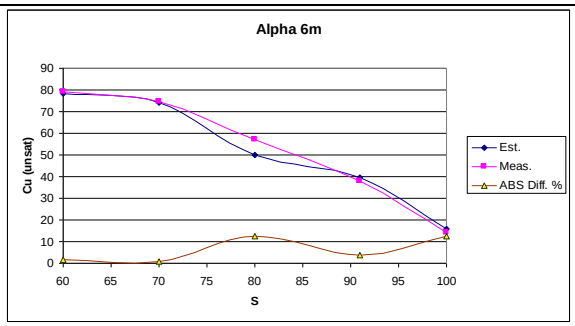

Figure 19. Comparison between estimated and measured shear stress values with different degree of saturation by α method at 6 m depth CBPN56.

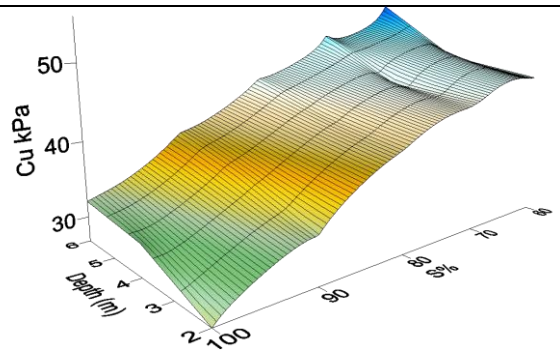

Figure 20. Surface among shear strength, depth and degree of saturation.

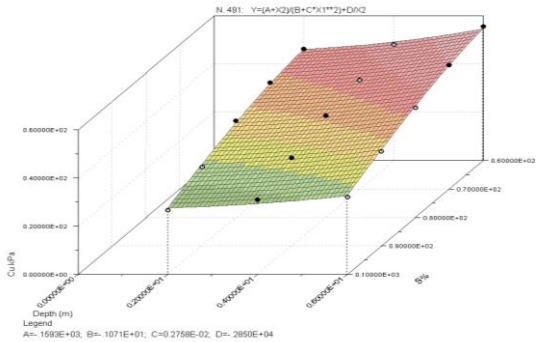

Figure 21. 3D-Surface among shear strength, depth and degree of saturation.

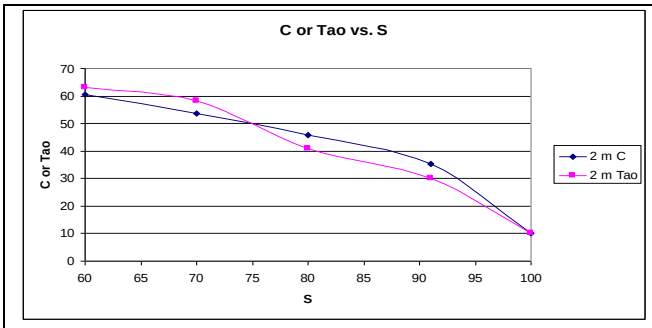

Figure 13. Relationship between (undrained shear strength, undrained shear stress) and degree of saturation at 2 m depth CBPN65.

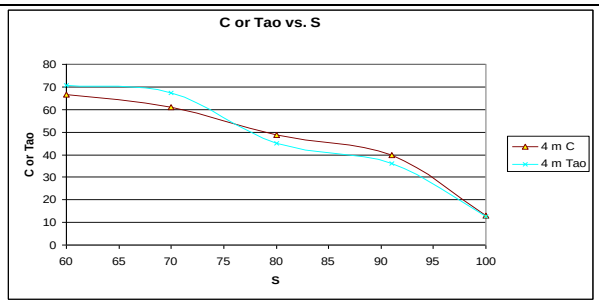

Figure 14. Relationship between (undrained shear strength, undrained shear stress) and degree of saturation at 4 m depth CBPN65.

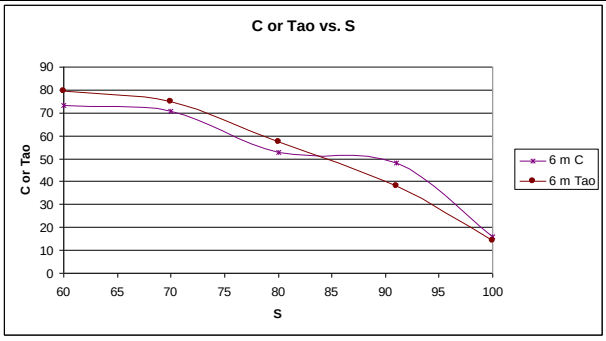

Figure 15. Relationship between (undrained shear strength, undrained shear stress) and degree of saturation at 6 m depth CBPN65.